Published in final edited form as:
Magn Reson Med. 2011 June ; 65(6): 1759–1767. doi:10.1002/mrm.22762.

Improved Diagnostic Accuracy of Breast MRI through Combined Apparent Diffusion Coefficients and Dynamic Contrast-Enhanced Kinetics

SC Partridge, PhD[1], **H Rahbar, MD**[1], **R Murthy, BS**[2], **X Chai, MS**[3], **BF Kurland, PhD**[3], **WB DeMartini, MD**[1], and **CD Lehman, MD PhD**[1]

[1]Department of Radiology, University of Washington, Seattle, WA

[2]Department of Bioengineering, University of Washington, Seattle, WA

[3]Division of Clinical Statistics, Fred Hutchinson Cancer Research Center, Seattle, WA

Abstract

This study investigated the relationship between apparent diffusion coefficient (ADC) measures and dynamic contrast-enhanced magnetic resonance imaging (DCE-MRI) kinetics in breast lesions, and evaluated the relative diagnostic value of each quantitative parameter. Seventy-seven women with 100 breast lesions (27 malignant and 73 benign) underwent both DCE-MRI and diffusion weighted MRI (DWI). DCE-MRI kinetic parameters included peak initial enhancement, predominant delayed kinetic curve type (persistent, plateau or washout), and worst delayed kinetic curve type (washout>plateau>persistent). Associations between ADC and DCE-MRI kinetic parameters and predictions of malignancy were evaluated. Results showed that ADC was significantly associated with predominant curve type (ADC was higher for lesions exhibiting predominantly persistent enhancement compared to those exhibiting predominantly washout or plateau, $p=0.006$), but was not significantly associated with peak initial enhancement or worst curve type ($p>0.05$). Univariate analysis showed significant differences between benign and malignant lesions in both ADC ($p<0.001$) and worst curve ($p=0.003$). In multivariate analysis, worst curve type and ADC were significant independent predictors of benign versus malignant outcome and in combination produced the highest area under the ROC curve (AUC = 0.85, AUC=0.78 with 5-fold cross-validation).

Keywords

breast cancer; diffusion-weighted imaging (DWI); dynamic contrast-enhanced MRI (DCE-MRI); apparent diffusion coefficient (ADC)

Introduction

Breast MRI has proven an important adjunct to mammography for breast imaging. In particular, dynamic contrast-enhanced MRI (DCE-MRI) is highly sensitive for breast cancer detection with a reported range of 88% - 100% and is the most sensitive modality for breast cancer detection in high risk women (1,2). Further, it has been shown to be more accurate than either mammography or ultrasound in determining extent of malignancy (3-5). Despite these strengths, the relatively moderate specificity of DCE-MRI, with a reported range of

Correspondence To: Savannah Partridge, PhD, Research Assistant Professor of Radiology, University of Washington School of Medicine, Seattle Cancer Care Alliance, 825 Eastlake Ave. E., G3-200, Seattle, WA 98109-1023, Phone: (206) 288-1306, Fax: (206) 288-6556, scp3@u.washington.edu.

68% - 96%, can present challenges by detecting a significant number of benign lesions that overlap in their features with malignancies based on current interpretation criteria (6-10). As a result, additional MRI techniques which may improve the specificity and positive predictive value of breast MRI could reduce morbidity, economic costs, and psychosocial costs associated with unnecessary biopsies.

Quantitative MRI techniques have been shown to improve the accuracy of breast MRI. Specifically, evaluating lesion kinetics on DCE-MRI can increase the specificity of breast MRI (11). More recently, several studies have demonstrated that diffusion-weighted imaging (DWI) techniques are useful in differentiating benign from malignant lesions based on apparent diffusion coefficient (ADC) measures (12-19). As DCE-MRI kinetics are related to differences in vascular volume and permeability (20,21), it is reasonable to expect that the sensitivity of DWI to biophysical characteristics such as cell density, membrane integrity, and microstructure (22) would provide unique and complementary information to that of DCE-MRI kinetics data. This is supported by recent studies showing that a combination of DWI and DCE-MRI characteristics can achieve high diagnostic accuracy (23,24) and that DWI can improve the diagnostic performance of conventional breast MRI (25,26).

To our knowledge, the correlation between DCE-MRI kinetics and ADC values has not been examined. Given the inherently different physiological properties that these two techniques measure, we hypothesize that ADC values and DCE-MRI kinetic parameters will provide complementary information that could potentially improve breast MRI specificity. Therefore, the purpose of this study was to investigate the relationship between ADC values and DCE-MRI kinetics in breast lesions and to evaluate the relative diagnostic value of each quantitative parameter alone and in combination.

Materials and Methods

Subjects and Lesions

This study was approved by our internal review board and compliant with the Health Insurance Portability and Accountability Act. We retrospectively reviewed consecutive breast DCE-MRI examinations performed between October 2005 and November 2006. Inclusion criteria for the study consisted of all breast lesions identified on MRI that were assigned a final Breast Imaging Reporting and Data System (BI-RADS) (27) assessment of 3 (probably benign), 4 (suspicious) or 5 (highly suggestive of malignancy) and had a complete automated kinetic synopses generated by a computer-aided assessment (CAE) program (CADstream™, Merge Healthcare, Hartland, WI). BI-RADS 6 lesions (biopsy-proven, known malignancies) were excluded. Benign versus malignant outcomes were determined based on results of biopsy or minimum 2-year follow-up by either MRI or linkage with the regional Cancer Surveillance System (CSS) tumor registry.

In all, 168 breast lesions with a final MRI assessment of BI-RADS 3, 4 or 5 and definitive outcome were identified on 129 consecutive DCE-MRI examinations in 128 women over the course of the study period. DWI was not performed in the MR examinations for 29 lesions due to time constraints. Fourteen lesions were excluded from the study because of technical problems with the DWI sequences resulting from patient motion (n = 13) or inadequate fat suppression (n= 1). Further, 25 lesions were excluded because they were not CAE-evaluable due to issues including motion misregistration, very small or discontiguous lesion morphology and/or extensive background parenchymal enhancement. Therefore, the final cohort included 100 lesions in 78 examinations in 77 women. Although there were differences in study inclusion criteria, the lesions in this study constituted a subgroup of the lesions that were included in a prior study to evaluate the diagnostic value of enhancement

kinetics (28) and another to characterize mammographically and clinically-occult lesions on DWI (29).

MRI Acquisition

MR imaging was performed on a GE LX 1.5T scanner using a dedicated 8-channel bilateral breast coil (General Electric Medical Systems, Milwaukee, WI). During the study period, two scanning protocols were used as clinical practice and technology evolved. Both protocols were in keeping with guidelines established by the International Breast MRI Consortium (IBMC) and by the ACR Imaging Network (ACRIN) MRI trials. Each MR examination included a T2-weighted fast spin echo sequence, T1-weighted non-fat suppressed sequence, T1-weighted DCE-MRI sequence with one pre-contrast and multiple post-contrast scans, and a DWI sequence. All scans were performed in the axial orientation.

DCE-MRI was acquired with a T1-weighted 3D fast spoiled gradient recalled echo sequence with parallel imaging (VIBRANT); TR/TE = 6.2/3 msec, flip angle = 10°, and field of view (FOV) = 32-38 cm. From October 2005 through June 2006 scans were performed with 2.2 mm slice thickness, 350 × 350 matrix, and five post-contrast acquisitions centered at 90, 180, 270, 360 and 450 seconds. From July 2006 through November 2006 three post-contrast acquisitions were performed with 1.6 mm slice thickness, 420 × 420 matrix, and three post-contrast acquisitions centered at 90, 270, and 450 seconds. The contrast agent administered was 0.1 mmol/kg-body weight Gd-DTPA (Omniscan, GE).

DWI was performed following the DCE-MRI acquisition using a diffusion-weighted echo planar imaging (EPI) sequence with parallel imaging (ASSET); reduction factor = 2, TR/TE = 7000/71.5 msec, 3 NEX, matrix = 192 × 192, FOV = 36 cm, slice thickness = 5 mm, and gap = 0. Diffusion gradients were applied in six directions with b = 0 and 600 s/mm^2, and the scan time was 2:40 min.

Image Analysis

DCE-MRI scans were prospectively interpreted by one of four fellowship-trained radiologists specializing in breast imaging. Enhancement kinetics were assessed using a computer-aided evaluation software (CADstream™), as previously described (28). Briefly, the kinetic parameters calculated for each lesion included (1) peak initial enhancement, defined as the greatest percent increase in signal intensity by the first post-contrast sequence, (2) predominant kinetic curve type, defined as that comprising the largest percentage of the lesion delayed enhancement (washout, plateau, or persistent), and (3) worst curve type, defined as the single ‘most suspicious’ kinetic curve type exhibited in the lesion (any washout > any plateau > any persistent). This information, as well as ACR BI-RADS assessments and recommendations and pathology results, was entered into the clinical database for our institution and later extracted for the purposes of this study. Because the DCE-MRI scans were evaluated prospectively, the radiologists were blinded to lesion outcomes at the time of interpretation.

The diffusion-weighted images were retrospectively analyzed offline by researchers blinded to lesion outcomes at the time of image analysis. Diffusion maps were created using in-house Java-based software incorporating ImageJ (National Institutes of Health, public domain) and JDTI (Daniel P. Barboriak Laboratory, Duke University School of Medicine, Durham, NC) image processing tools. ADC maps were created from the spatially registered diffusion weighted images by

$$ADC = -\frac{1}{b}\ln\left(\frac{S_{DWI}}{S_0}\right) \quad [1]$$

where S_{DWI} is the combined DWI (geometric average of individual b = 600 s/mm^2 diffusion-weighted images), and S_0 is the T2-weighted b = 0 s/mm^2 reference image.

Lesions were identified from the DCE-MRI images based on description in the clinical radiology reports. A region of interest (ROI) was defined for each lesion at the corresponding location on the combined DWI (S_{DWI}) series to include the area of hyperintensity. The ROI was drawn free-hand to encompass as much of the abnormality as possible while staying within the border of the hyperintense region. Care was taken to avoid non-enhancing regions of high T2 within a lesion, such as cyst, hematoma, or necrosis, by verifying the ROI against the T2-weighted (b = 0 s/mm^2) image and ADC map. In the case that a lesion was not hyperintense on DWI, the ROI was drawn at the corresponding location and size as reflected on DCE-MRI. The lesion ADC value was calculated as the mean of the voxels in the ROI for each lesion.

Statistical Analysis

Associations between ADC and DCE-MRI kinetic variables and predictions of malignancy were evaluated by generalized estimating equations (GEE) so that standard errors would account for multiple lesions in the same patient (30). All tests were two-sided and model assumptions were checked using both influence statistics and visual inspection. The predictive abilities of the models were described using the area under the receiver operating characteristic curve (AUC), which is equivalent to the concordance measure c for logistic regression (or GEE with independence working correlation). Differences in AUC were assessed via pairwise ROC curve comparison (31). The AUC for the final multivariate model was also computed using predicted values from 5-fold cross-validation (32) to ensure that model assessment (AUC) was not conducted on precisely the same data as used for model development. Analyses were conducted using R version 2.8.1 (R Foundation for Statistical Computing, Vienna, Austria), SAS/STAT software, version 9.1 (SAS Institute, Inc., Cary, NC) and Medcalc version 10.4.5.0 (Medcalc Software, Mariakerke, Belgium).

Results

One hundred lesions in 77 women were evaluated for the study. Subjects ranged in age from 22 to 85 years (median, 49 years). The clinical indications for the examinations were high risk screening in 40/78 (52%), evaluation of extent of disease in patients with a new diagnosis of breast cancer in 33/78 (42%) and problem solving in 5/78 (6%). The study lesions detected in newly diagnosed cancer/evaluate extent of disease patients constituted additional lesions distinct from the known, biopsy proven cancers.

Of the 100 lesions in the study, and 27 (27%) were biopsy-proven malignancies and 73 (73%) were benign as determined by biopsy (n=44) or follow-up (n=29). Lesion characteristics are reported in Table 1. Nine of 27 malignancies were ductal carcinoma in situ (DCIS) and 18 were invasive carcinoma. Of the benign lesions that were biopsied, the most frequent histologies were fibroadenoma (n=9), atypical ductal hyperplasia (ADH, n=6), psuedoangiomatous stromal hyperplasia (PASH, n=5), focal fibrosis (n=4), and fibrocystic changes (n=4). Lesion sizes, as defined by the longest dimension on DCE-MRI, ranged from 0.3 to 8.3 cm (median, 1.0 cm). The average ADC (± one standard deviation) was 1.60 $\pm 0.43 \times 10^{-3}$ mm^2/s; the average peak initial enhancement on DCE-MRI was 145 ± 50 %. The large majority of lesions (88%) demonstrated persistent enhancement as the

predominant curve type. By worst curve assessment, 51/100 (51%) lesions exhibited washout, 31/100 (31%) exhibited plateau, and 18 of 100 (18%) exhibited only persistent enhancement. Benign and malignant lesion characteristics are compared in Table 2.

Small sample sizes precluded statistical comparisons of DWI and DCE-MRI characteristics between benign and malignant subtypes. By observational analysis, invasive lobular carcinoma (ILC) demonstrated less suspicious kinetics compared to invasive ductal carcinoma (IDC): all six ILC exhibited persistent enhancement as the predominant kinetic pattern (compared to 75% of IDC) and only 66% exhibited washout as the worst curve type (compared to 83% of IDC). On the other hand, there was little difference in ADC between ILC (mean, 1.28×10^{-3} mm^2/s) and IDC (mean, 1.24×10^{-3} mm^2/s). DCIS was not significantly different than invasive disease by either DCE-MRI kinetics or ADC. Of the most common benign histologies in the cohort, ADH and PASH exhibited lower mean ADC values (1.53 and 1.59×10^{-3} mm^2/s, respectively) compared to fibroadenomas (mean, 1.85×10^{-3} mm^2/s), while there was little difference in DCE-MRI kinetics between the three benign subtypes.

Univariate Differences Between Benign and Malignant Lesions

Table 2 summarizes univariate comparisons between benign and malignant lesions. Compared to benign lesions, malignancies exhibited lower mean ADC ($p < 0.001$), Figure 1a, and more often exhibited washout as the worst curve type ($p=0.003$), such as the example in Figure 2. Malignant lesions also tended to exhibit predominant curve types of washout or plateau more often than benign lesions ($p = 0.047$). However, there were exceptions, such as malignancies that did not exhibit any washout (n=6/27), and benign lesions displaying washout (n=30/73) and/or low ADC values (ADC<1.8 mm^2/s, n=46/73); several examples are shown in Figure 3. No significant differences were observed between benign and malignant lesions for peak initial enhancement ($p = 0.586$, Figure 1b).

Association Between ADC and DCE-MRI Kinetics

ADC values and DCE-MRI kinetic parameters were compared for all lesions using GEE, Table 3. There was no significant correlation between ADC and peak initial enhancement (Figure 4, $p=0.182$). ADC was significantly higher for lesions exhibiting predominantly persistent enhancement (mean ADC, $1.64 \pm 0.44 \times 10^{-3}$ mm^2/s) compared to those exhibiting predominantly washout or plateau enhancement (mean ADC, $1.39 \pm 0.30 \times 10^{-3}$ mm^2/s, $p=0.006$). As seen in Figure 5, most lesions had predominately persistent enhancement, so pairwise comparisons with predominantly washout or plateau enhancement were not examined separately. For the worst curve, lesions with persistent delayed enhancement (mean ADC, $1.78 \pm 0.47 \times 10^{-3}$ mm^2/s) showed a trend to have higher ADC than those exhibiting washout (mean ADC, $1.55 \pm 0.43 \times 10^{-3}$ mm^2/s, $p= 0.09$), but did not differ from those exhibiting plateau delayed enhancement (mean ADC, $1.60 \pm 0.41 \times 10^{-3}$ mm^2/s, $p = 0.180$).

Multivariate Analysis to Discriminate Lesions

In a GEE model with binary outcome (malignancy) and independence working correlation, ADC and worst curve kinetics type were independent predictors of malignancy ($p<0.001$ and $p=0.024$, respectively). Table 4 summarizes predicted probabilities of malignancy based on the multivariable GEE model. At the 75^{th} percentile observed for ADC (1.86×10^{-3} mm^2/s), the predicted probability of malignancy was only 4% for persistent worst curve and 3% for plateau, but was 15% for washout. The respective probabilities of malignancy for persistent, plateau, and washout delayed worst curve kinetics at the 25^{th} percentile for ADC (1.26×10^{-3} mm^2/s) were 27%, 22%, and 62%. Of the 100 lesions, 24% had predicted

probability of malignancy less than 5% (with one malignancy among the 24), and 36% had predicted probability of malignancy greater than 33% (with a 21/36 = 58% malignancy rate).

The model incorporating ADC and worst curve kinetics produced higher area under the ROC curve (AUC = 0.85, SE= 0.04, 95% CI = 0.77, 0.93) than either ADC (AUC = 0.79, SE= 0.05, 95% CI = 0.70, 0.87, p=0.05) or worst curve alone (AUC = 0.69, SE= 0.06, 95% CI = 0.59, 0.78, p=0.007), Figure 6. The AUC was attenuated but retained significance when 5-fold cross-validation was applied, fitting the model to 4/5 of the data at a time to create predicted probabilities of malignancy for the other 1/5 (AUC = 0.78, SE=0.06, 95% CI = 0.66, 0.90). The difference in AUC between ADC alone and worst-curve alone was not statistically significant (p=0.161).

Discussion

Our results suggest that the apparent diffusion coefficient (ADC) measured by diffusion weighted imaging (DWI) provides distinct and complementary information to dynamic contrast-enhanced MRI (DCE-MRI) kinetics for characterizing breast lesions and in combination may improve diagnostic accuracy. DWI provides information on the intrinsic tissue properties affecting the microscopic mobility of water (due to Brownian motion). ADC has been linked to tumor lesion aggressiveness and tumor response in oncologic imaging (33). The tissue properties affecting DWI are distinct from that of DCE-MRI, which relies on differences in tissue vascularity reflected by enhancement kinetics to identify breast malignancies. While DWI is not yet routinely used for clinical breast imaging, previous research studies have reported differences in ADC between benign and malignant breast lesions (12-19) and high diagnostic accuracy through a multivariate combination of ADC and DCE-MRI features (23,24).

Our study is the first to correlate quantitative DWI and CAE-generated DCE-MRI kinetic characteristics, and demonstrates that lower lesion ADC values (representing higher cellularity) are associated with more suspicious kinetics. Furthermore, multivariate analysis showed ADC and worst curve type to be significant independent predictors of benign versus malignant lesions and confirmed that DWI provided complementary information to DCE-MRI kinetics. The multivariate model provided significantly higher diagnostic performance (AUC=0.85) than worst curve kinetics (AUC=0.69) or ADC (AUC =0.79) alone. The large range of predicted probabilities of malignancy over worst curve kinetics and ADC values demonstrates that combined DCE-MRI and DWI-MRI information shows potential for increasing the specificity of breast MRI. These findings are in agreement with other recent studies demonstrating that incorporating DWI into the clinical breast MRI assessment can help to improve diagnostic performance (25,26). Future larger studies will enable evaluation of model performance for specific lesion subgroups, such as masses versus non-mass lesions and for different benign and malignant histologies.

Practical considerations of including DWI in routine breast MRI examinations are the additional scan time (on the order of 3 minutes) and radiologists' time to review the DWI images. Although extensive cost-benefit analysis was not performed in this study, the improved specificity would almost certainly offset these drawbacks in the long term by potentially decreasing the number of unnecessary biopsies. Further, this would have the clinically desirable benefit of a reduction in patient morbidity associated with procedures.

In addition, the comparable diagnostic accuracies of ADC alone and worst-curve alone suggests that DWI could have potential benefit in patients for whom contrast (Gd-DTPA) is contraindicated such as those with renal insufficiency. This is particularly salient in view of recent evidence that reducing contrast doses in such patients could significantly decrease

enhancement of some breast cancers (34). Further investigation comparing ADC to DCE-MRI is certainly needed, however, particularly in view of the fact that in this study all lesions were identified first with DCE-MRI and BI-RADs 2 lesions were excluded.

Our study has several limitations. The primary aim was to evaluate the association between quantitative tumor characteristics on DWI and DCE-MRI, and we therefore did not include the morphologic features of the lesions in the analysis, which can further improve the diagnostic accuracy of conventional breast MRI (35). Although they were not excluded, the study did not include any mucinous carcinomas, which tend to exhibit persistent enhancement and high ADC and could present a challenge for the model. ROIs were drawn manually on DWI images with reference to the DCE-MRI images. Automated segmentation of ADC maps based on DCE-MRI abnormalities was not possible due to the spatial distortions inherent to EPI-based DWI datasets (caused by B0 field inhomogeneities). However, reducing the spatial distortion of breast DWI is an active area of research involving new non-EPI pulse sequences (36,37) and post-processing correction techniques (38) and may enable direct voxel to voxel comparison of DWI and DCE-MRI and multi-parametric mapping in future work. DWI was performed with a diffusion sensitization of b=600 s/mm^2. Higher b values and field strength (3 Tesla) may further improve the discrimination of breast lesions on DWI (39,40). Furthermore, ADC was calculated from only two b-values, with b_{min} = 0 s/mm^2. Others have shown that the signal loss from diffusion in vivo is driven by both perfusion and diffusion, with the changes at low b values dominated by perfusion and the higher values characterizing intra- and extra-cellular diffusion (17,40,41). Although our simple approach has the advantage of being readily translatable to the clinic, calculation of ADC using a greater number of b-values and nonzero b_{min} would enable a more detailed comparison of DCE kinetic profiles in the fast and slow diffusion regimes and further extend knowledge in this area. In our study, DWI was performed after injection of a gadolinium-based contrast agent. While several prior studies have not shown a significant effect on ADC following administration of a contrast agent (16,42-44), it may be preferable to acquire DWI sequences prior to contrast injection to avoid any possible confounding effects.

In conclusion, we found that ADC provided unique and complementary information to DCE-MRI kinetic parameters for characterizing a variety of breast lesions and may improve the diagnostic accuracy of breast MRI. Future prospective studies are needed to determine the optimal way to incorporate ADC into the standard breast MRI assessment to reduce the number of unnecessary biopsies performed as a result of breast MRI

Acknowledgments

Grant Sponsors: Susan G. Komen for the Cure grant BCTR0600618, NCI Cancer Center Support Grant (Comprehensive) - Biostatistics Shared Resource P30 CA015704, and Institute of Translational Health Sciences grant 1 UL1 RR 025014-01.

References

1. Saslow D, Boetes C, Burke W, Harms S, Leach MO, Lehman CD, Morris E, Pisano E, Schnall M, Sener S, Smith RA, Warner E, Yaffe M, Andrews KS, Russell CA. American Cancer Society guidelines for breast screening with MRI as an adjunct to mammography. CA Cancer J Clin. 2007; 57(2):75–89. [PubMed: 17392385]
2. Kriege M, Brekelmans CT, Boetes C, Besnard PE, Zonderland HM, Obdeijn IM, Manoliu RA, Kok T, Peterse H, Tilanus-Linthorst MM, Muller SH, Meijer S, Oosterwijk JC, Beex LV, Tollenaar RA, de Koning HJ, Rutgers EJ, Klijn JG. Efficacy of MRI and mammography for breast-cancer screening in women with a familial or genetic predisposition. N Engl J Med. 2004; 351(5):427–437. [PubMed: 15282350]

3. Schnall MD, Blume J, Bluemke DA, Deangelis GA, Debruhl N, Harms S, Heywang-Kobrunner SH, Hylton N, Kuhl CK, Pisano ED, Causer P, Schnitt SJ, Smazal SF, Stelling CB, Lehman C, Weatherall PT, Gatsonis CA. MRI detection of distinct incidental cancer in women with primary breast cancer studied in IBMC 6883. J Surg Oncol. 2005; 92(1):32–38. [PubMed: 16180227]
4. Lehman CD, Gatsonis C, Kuhl CK, Hendrick RE, Pisano ED, Hanna L, Peacock S, Smazal SF, Maki DD, Julian TB, DePeri ER, Bluemke DA, Schnall MD. MRI evaluation of the contralateral breast in women with recently diagnosed breast cancer. N Engl J Med. 2007; 356(13):1295–1303. [PubMed: 17392300]
5. Hollingsworth AB, Stough RG, O'Dell CA, Brekke CE. Breast magnetic resonance imaging for preoperative locoregional staging. Am J Surg. 2008; 196(3):389–397. [PubMed: 18436185]
6. Bluemke DA, Gatsonis CA, Chen MH, DeAngelis GA, DeBruhl N, Harms S, Heywang-Kobrunner SH, Hylton N, Kuhl CK, Lehman C, Pisano ED, Causer P, Schnitt SJ, Smazal SF, Stelling CB, Weatherall PT, Schnall MD. Magnetic resonance imaging of the breast prior to biopsy. Jama. 2004; 292(22):2735–2742. [PubMed: 15585733]
7. Huang W, Fisher PR, Dulaimy K, Tudorica LA, O'Hea B, Button TM. Detection of breast malignancy: diagnostic MR protocol for improved specificity. Radiology. 2004; 232(2):585–591. [PubMed: 15205478]
8. Kinkel K, Helbich TH, Esserman LJ, Barclay J, Schwerin EH, Sickles EA, Hylton NM. Dynamic high-spatial-resolution MR imaging of suspicious breast lesions: diagnostic criteria and interobserver variability. AJR Am J Roentgenol. 2000; 175(1):35–43. [PubMed: 10882243]
9. Nunes LW, Schnall MD, Orel SG, Hochman MG, Langlotz CP, Reynolds CA, Torosian MH. Breast MR imaging: interpretation model. Radiology. 1997; 202(3):833–841. [PubMed: 9051042]
10. Warren RM, Pointon L, Thompson D, Hoff R, Gilbert FJ, Padhani A, Easton D, Lakhani SR, Leach MO. Reading protocol for dynamic contrast-enhanced MR images of the breast: sensitivity and specificity analysis. Radiology. 2005; 236(3):779–788. [PubMed: 16118160]
11. Kuhl CK, Mielcareck P, Klaschik S, Leutner C, Wardelmann E, Gieseke J, Schild HH. Dynamic breast MR imaging: are signal intensity time course data useful for differential diagnosis of enhancing lesions? Radiology. 1999; 211(1):101–110. [PubMed: 10189459]
12. Guo Y, Cai YQ, Cai ZL, Gao YG, An NY, Ma L, Mahankali S, Gao JH. Differentiation of clinically benign and malignant breast lesions using diffusion-weighted imaging. J Magn Reson Imaging. 2002; 16(2):172–178. [PubMed: 12203765]
13. Hatakenaka M, Soeda H, Yabuuchi H, Matsuo Y, Kamitani T, Oda Y, Tsuneyoshi M, Honda H. Apparent diffusion coefficients of breast tumors: clinical application. Magn Reson Med Sci. 2008; 7(1):23–29. [PubMed: 18460845]
14. Kinoshita T, Yashiro N, Ihara N, Funatu H, Fukuma E, Narita M. Diffusion-weighted half-Fourier single-shot turbo spin echo imaging in breast tumors: differentiation of invasive ductal carcinoma from fibroadenoma. J Comput Assist Tomogr. 2002; 26(6):1042–1046. [PubMed: 12488758]
15. Marini C, Iacconi C, Giannelli M, Cilotti A, Moretti M, Bartolozzi C. Quantitative diffusion-weighted MR imaging in the differential diagnosis of breast lesion. Eur Radiol. 2007; 17(10): 2646–2655. [PubMed: 17356840]
16. Rubesova E, Grell AS, De Maertelaer V, Metens T, Chao SL, Lemort M. Quantitative diffusion imaging in breast cancer: a clinical prospective study. J Magn Reson Imaging. 2006; 24(2):319–324. [PubMed: 16786565]
17. Sinha S, Lucas-Quesada FA, Sinha U, DeBruhl N, Bassett LW. In vivo diffusion-weighted MRI of the breast: potential for lesion characterization. J Magn Reson Imaging. 2002; 15(6):693–704. [PubMed: 12112520]
18. Wenkel E, Geppert C, Schulz-Wendtland R, Uder M, Kiefer B, Bautz W, Janka R. Diffusion weighted imaging in breast MRI: comparison of two different pulse sequences. Acad Radiol. 2007; 14(9):1077–1083. [PubMed: 17707315]
19. Woodhams R, Matsunaga K, Kan S, Hata H, Ozaki M, Iwabuchi K, Kuranami M, Watanabe M, Hayakawa K. ADC mapping of benign and malignant breast tumors. Magn Reson Med Sci. 2005; 4(1):35–42. [PubMed: 16127252]

20. Esserman L, Hylton N, George T, Weidner N. Contrast-Enhanced Magnetic Resonance Imaging to Assess Tumor Histopathology and Angiogenesis in Breast Carcinoma. Breast J. 1999; 5(1):13–21. [PubMed: 11348250]
21. Knopp MV, Weiss E, Sinn HP, Mattern J, Junkermann H, Radeleff J, Magener A, Brix G, Delorme S, Zuna I, van Kaick G. Pathophysiologic basis of contrast enhancement in breast tumors. J Magn Reson Imaging. 1999; 10(3):260–266. [PubMed: 10508285]
22. Le Bihan D, Turner R, Douek P, Patronas N. Diffusion MR imaging: clinical applications. AJR Am J Roentgenol. 1992; 159(3):591–599. [PubMed: 1503032]
23. Yabuuchi H, Matsuo Y, Okafuji T, Kamitani T, Soeda H, Setoguchi T, Sakai S, Hatakenaka M, Kubo M, Sadanaga N, Yamamoto H, Honda H. Enhanced mass on contrast-enhanced breast MR imaging: Lesion characterization using combination of dynamic contrast-enhanced and diffusion-weighted MR images. J Magn Reson Imaging. 2008; 28(5):1157–1165. [PubMed: 18972357]
24. Yabuuchi H, Matsuo Y, Kamitani T, Setoguchi T, Okafuji T, Soeda H, Sakai S, Hatakenaka M, Kubo M, Tokunaga E, Yamamoto H, Honda H. Non-mass-like enhancement on contrast-enhanced breast MR imaging: Lesion characterization using combination of dynamic contrast-enhanced and diffusion-weighted MR images. Eur J Radiol. 2009
25. El Khouli RH, Jacobs MA, Mezban SD, Huang P, Kamel IR, Macura KJ, Bluemke DA. Diffusion-weighted imaging improves the diagnostic accuracy of conventional 3.0-T breast MR imaging. Radiology. 2010; 256(1):64–73. [PubMed: 20574085]
26. Partridge SC, DeMartini WB, Kurland BF, Eby PR, White SW, Lehman CD. Quantitative diffusion-weighted imaging as an adjunct to conventional breast MRI for improved positive predictive value. AJR Am J Roentgenol. 2009; 193(6):1716–1722. [PubMed: 19933670]
27. American College of Radiology (ACR) Breast imaging reporting and data system atlas (BI-RADS Atlas). Reston, VA: 2003.
28. Wang LC, DeMartini WB, Partridge SC, Peacock S, Lehman CD. MRI-detected suspicious breast lesions: predictive values of kinetic features measured by computer-aided evaluation. AJR Am J Roentgenol. 2009; 193(3):826–831. [PubMed: 19696298]
29. Partridge SC, Demartini WB, Kurland BF, Eby PR, White SW, Lehman CD. Differential diagnosis of mammographically and clinically occult breast lesions on diffusion-weighted MRI. J Magn Reson Imaging. 2010; 31(3):562–570. [PubMed: 20187198]
30. Levine D, Bankier AA, Halpern EF. Submissions to Radiology: Our top 10 list of statistical errors. Radiology. 2009; 253:288–290.
31. Hanley JA, McNeil BJ. A method of comparing the areas under receiver operating characteristic curves derived from the same cases. Radiology. 1983; 148(3):839–843. [PubMed: 6878708]
32. Gonen, M. Analyzing receiver operating characteristic curves with SAS. SAS Publishing; 2008.
33. Padhani AR, Liu G, Koh DM, Chenevert TL, Thoeny HC, Takahara T, Dzik-Jurasz A, Ross BD, Van Cauteren M, Collins D, Hammoud DA, Rustin GJ, Taouli B, Choyke PL. Diffusion-weighted magnetic resonance imaging as a cancer biomarker: consensus and recommendations. Neoplasia. 2009; 11(2):102–125. [PubMed: 19186405]
34. Jansen SA, Fan X, Yang C, Shimauchi A, Karczmar G, Newstead GM. Relating Dose of Contrast Media Administered to Uptake and Washout of Malignant Lesions on DCEMRI of the Breast(1). Acad Radiol. 2009
35. Ei Khouli RH, Jacobs MA, Mezban SD, Huang P, Kamel IR, Macura KJ, Bluemke DA. Diffusion-weighted imaging improves the diagnostic accuracy of conventional 3.0-T breast MR imaging. Radiology. 256(1):64–73. [PubMed: 20574085]
36. Veldhuis, WB.; Liu, C.; Bammer, R.; Daniel, BL.; Mosely, ME. High-resolution, fat-suppressed, diffusion-weighted MRI of the breast using a self-navigated multi-shot technique. Honolulu, HI: 2009. p. 2098
37. Lin, C.; Geppert, C.; Stemmer, A.; Schultze-Haakh, H.; Majidi, SS.; Kipfer, HD. Diffusion weighted imaging of the breast at 3.0T with BLADE-TSE: Initial Experience. Honolulu, HI: 2009. p. 4119
38. Yankeelov, T.; Gatenby, JC.; Welch, EB.; Chakravarthy, B.; Freehardt, D.; Mayer, I.; Kelly, M.; Meszoely, I.; Gore, J. Towards practical breast diffusion tensor imaging at 3.0T in the clinical setting. Honolulu, HI: 2009. p. 2131

39. Dudink J, Larkman DJ, Kapellou O, Boardman JP, Allsop JM, Cowan FM, Hajnal JV, Edwards AD, Rutherford MA, Counsell SJ. High b-value diffusion tensor imaging of the neonatal brain at 3T. AJNR Am J Neuroradiol. 2008; 29(10):1966–1972. [PubMed: 18687746]
40. Bogner W, Gruber S, Pinker K, Grabner G, Stadlbauer A, Weber M, Moser E, Helbich TH, Trattnig S. Diffusion-weighted MR for differentiation of breast lesions at 3.0 T: how does selection of diffusion protocols affect diagnosis? Radiology. 2009; 253(2):341–351. [PubMed: 19703869]
41. Le Bihan D, Breton E, Lallemand D, Aubin ML, Vignaud J, Laval-Jeantet M. Separation of diffusion and perfusion in intravoxel incoherent motion MR imaging. Radiology. 1988; 168(2): 497–505. [PubMed: 3393671]
42. Ogura A, Hayakawa K, Miyati T, Maeda F. The effect of susceptibility of gadolinium contrast media on diffusion-weighted imaging and the apparent diffusion coefficient. Acad Radiol. 2008; 15(7):867–872. [PubMed: 18572122]
43. Fitzek C, Mentzel HJ, Fitzek S, Sauner D, Kaiser WA, Reichenbach JR. Echoplanar diffusion-weighted MRI with intravenous gadolinium-DTPA. Neuroradiology. 2003; 45(9):592–597. [PubMed: 12923668]
44. Chen G, Jespersen SN, Pedersen M, Pang Q, Horsman MR, Stodkilde-Jorgensen H. Intravenous administration of Gd-DTPA prior to DWI does not affect the apparent diffusion constant. Magn Reson Imaging. 2005; 23(5):685–689. [PubMed: 16051044]

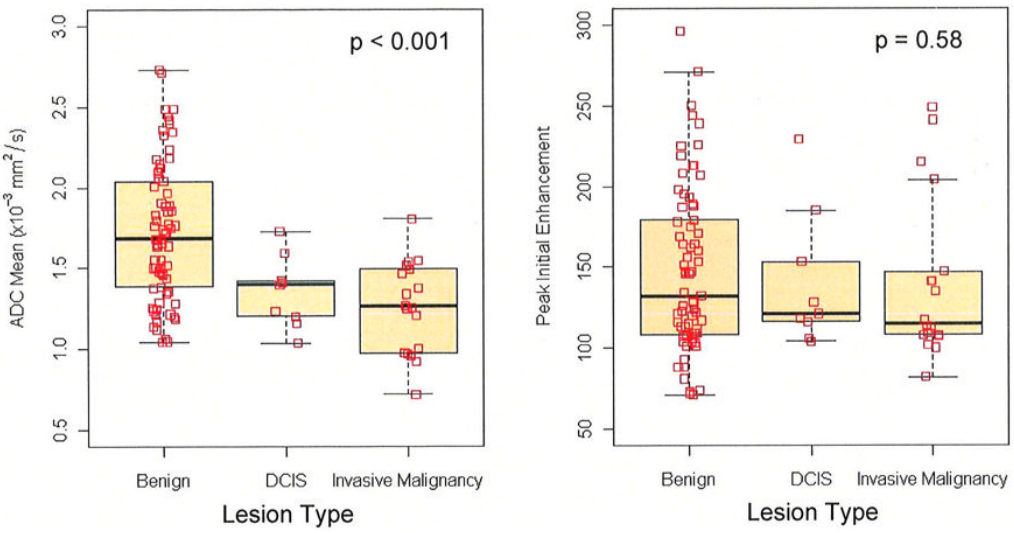

Figure 1.

Boxplots of DWI-MRI ADC and PE values versus diagnosis categories (benign, DCIS, and invasive carcinoma). P values are given for GEE test of differences between benign and malignant (DCIS and invasive carcinoma).

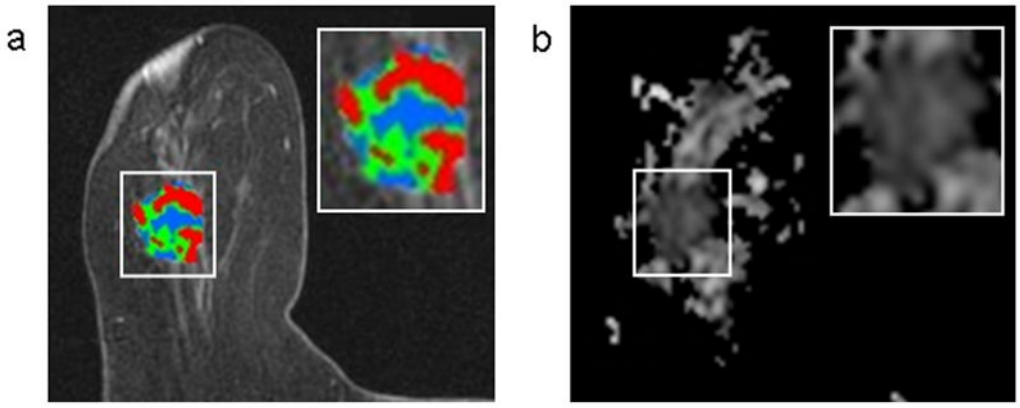

Figure 2.
A 2.2 cm enhancing invasive ductal carcinoma detected in an 85-year-old woman who underwent breast MRI for a suspicious palpable mass in the right breast. DCE-MRI showed a lobular mass with spiculated margins that demonstrated significant washout (shown in red) (a). The mass exhibited low ADC (mean ADC, 1.25 $\times 10^{-3}$ mm^2/s) on DWI (b).

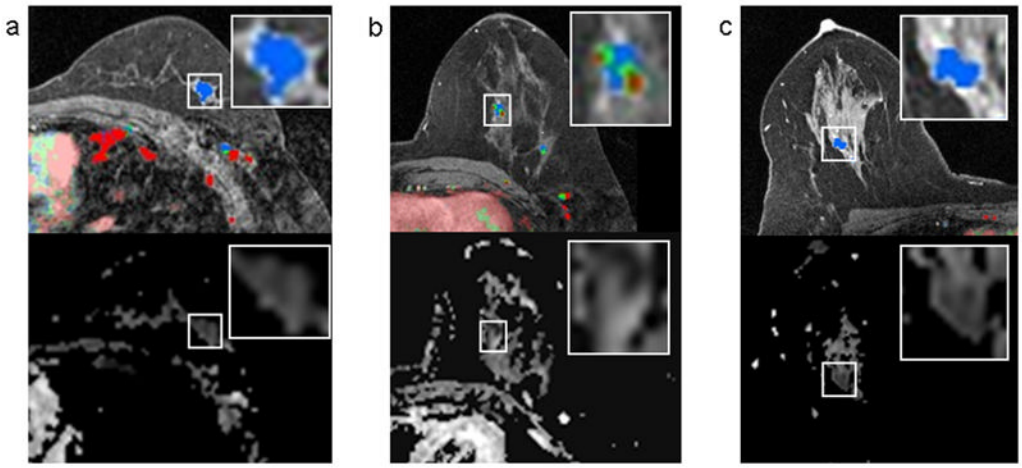

Figure 3.

Several lesion examples where DCE-MRI and DWI suggested different levels of suspicion. DCE-MR images are shown on the top row and corresponding ADC maps are shown below. In each case, the lesion of interest is delineated by a box on both images and enlarged for clarity (boxes do not represent the ROIs, which were manually drawn within lesion borders as described in the methods). A 1.1 cm invasive ductal carcinoma in a 59 year-old woman that demonstrated only persistent enhancement on DCE-MRI with no washout, but exhibited a low ADC value on DWI (mean ADC, 1.34×10^{-3} mm^2/s) (a). A 1.0 cm benign papilloma detected in a 41 year-old woman that demonstrated concerning washout (red), but exhibited high ADC (mean ADC, 2.04×10^{-3} mm^2/s) (b). A 2.6 cm region of benign fibrocystic change detected in a 43-year old woman that demonstrated no washout on DCE-MRI, but exhibited suspiciously reduced diffusivity, with low ADC values (mean, 1.04×10^{-3} mm^2/s).

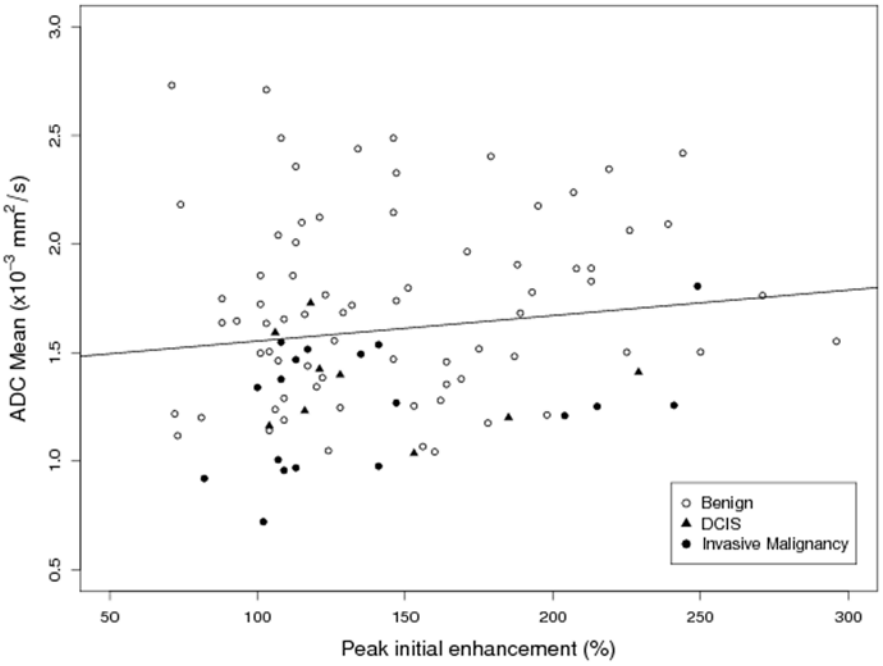

Figure 4.
Scatterplot of ADC mean versus peak enhancement by lesion class, with GEE fitted line (slope = 0.0012, p = 0.182). No significant association was observed between lesion ADC and peak enhancement.

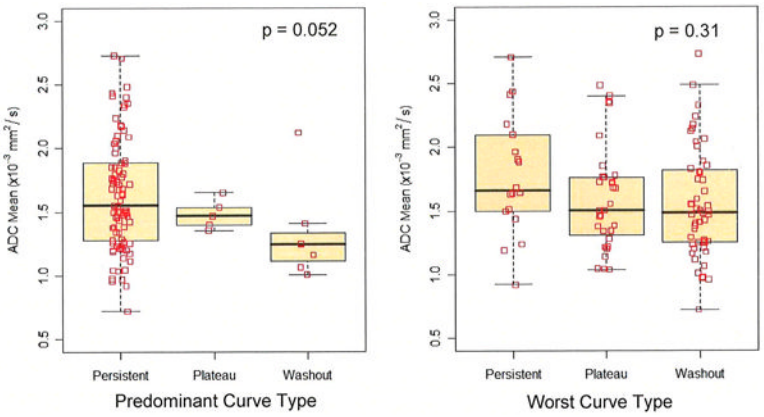

Figure 5.

Boxplots of DWI ADC values versus DCE-MRI delayed phase kinetics (predominant and worst curve type), n=100 lesions. P values are given for GEE test of overall differences between curve type categories (persistent, plateau, and washout).

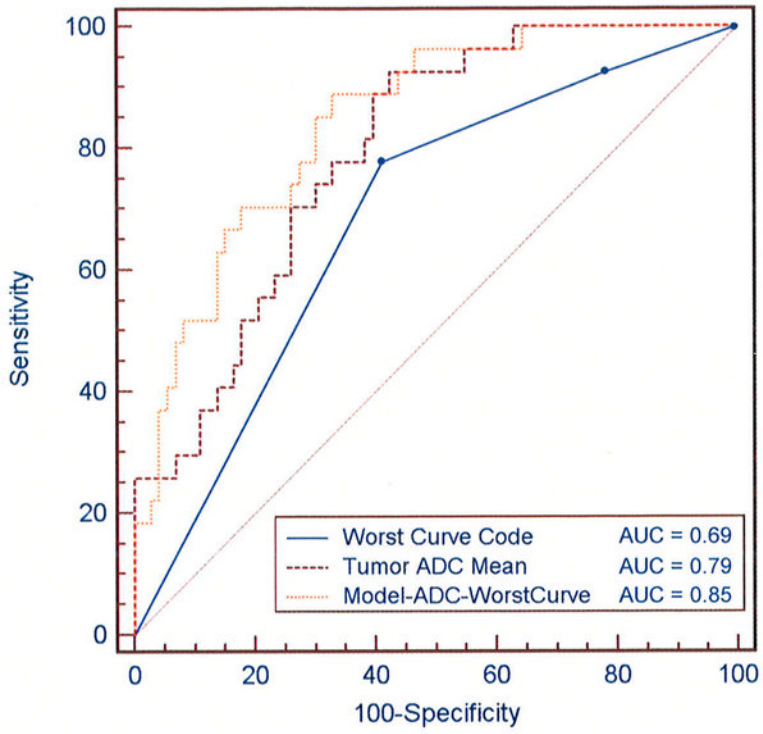

Figure 6.

ROC comparisons of ADC, DCE-MRI worst curve, and a model combining the two parameters for discriminating benign and malignant lesions. Curves represent the diagnostic performance of logistic regression models for (1) worst curve alone: y = 1.16 + 0.81*worst curve, where worst curve has value 1 for washout or 0 for no washout (persistent or plateau), (2) ADC alone: y = -4.36 + 3.63*ADC, where ADC is in units $\times 10^{-3}$ mm^2/s, and (3) Combined ADC and worst curve: y = -4.28 + 3.69*ADC +0.84*worst curve. The area under the curve (AUC) is calculated for each model for comparison of diagnostic performance.

Table 1

Lesion characteristics (n = 100).

	n	(%)
Size*		
≤ 5 mm	13	13%
6 mm - 1 cm	38	38%
1.1 cm - 2 cm	22	22%
> 2 cm	27	27%
BI-RADS Assessment		
3	23	23%
4	66	66%
5	11	11%
Enhancement Type		
Focus	8	8%
Mass	61	61%
NMLE	31	31%
Source of Diagnosis		
Biopsy	71	71%
MRI follow-up	19	19%
Linkage with tumor registry	10	10%
Lesion Diagnosis		
Benign	73	73%
DCIS	9	9%
Invasive Malignancy	18	18%
IDC	12/18	
ILC	6/18	

Abbreviations: BI-RADS = Breast Imaging Reporting and Data System, NMLE = non-mass-like-enhancement, DCIS = ductal carcinoma in situ, IDC = invasive ductal carcinoma, ILC = invasive lobular carcinoma

*Size determined by longest diameter on DCE-MRI

Table 2

Univariate comparisons between benign and malignant lesions.

	Malignant (n=27) Mean ± SD or n (%)	Benign lesions (n=73) Mean ± SD or n (%)	p-value
ADC ($\times 10^{-3}$ mm^2/s)	1.29 ± 0.26	1.72 ± 0.43	<0.001
Peak Initial Enhancement (%)	140 ± 47	147 ± 51	0.586
Predominant Kinetic Curve Type			0.047
Persistent	21 (78%)	67 (92%)	
Plateau	2 (7%)	3 (4%)	
Washout	4 (15%)	3 (4%)	
Worst Curve Type			0.003
Persistent	2 (7%)	16 (22%)	
Plateau	4 (15%)	27 (37%)	
Washout	21 (78%)	30 (41%)	

Note: P-values were from GEE with “independence” correlation structure

Abbreviations: ADC = apparent diffusion coefficient, SD = standard deviation

Table 3

Association between ADC and DCE-MRI kinetic parameters for 100 lesions.

	n (%)	ADC ($\times 10^{-3}$ mm^2/s) (Mean ± SD)	Association with ADC (p-value)
Peak Initial Enhancement (%)			0.182*
50-99	9 (9%)	1.60 ± 0.58	
100-199	74 (74%)	1.57 ± 0.43	
>200	17 (17%)	1.77 ± 0.38	
Predominant Curve Type			0.052**
Persistent	88 (88%)	1.64 ± 0.44	
Plateau	5 (5%)	1.48 ± 0.12	
Washout	7 (7%)	1.32 ± 0.38	
Worst Curve Type			0.310**
Persistent	18 (18%)	1.78 ± 0.47	
Plateau	31 (31%)	1.60 ± 0.41	
Washout	51 (51%)	1.55 ± 0.43	

* P-value from generalized estimating equations (GEE) with "independence" correlation structure, analogous to Student's t test with sandwich standard errors to adjust for multiple lesions in some patients.

** P-value represents global factor effect, determined by score statistics for type 3 GEE analysis.

Table 4

Probability of malignancy for different ADC values in the three DCE-MRI worst curve categories.

		Worst Curve Type					
		Persistent		Plateau		Washout	
ADC Quartile	ADC Range ($\times 10^{-3}$ mm^2/s)	n	Probability of Malignancy	n	Probability of Malignancy	n	Probability of Malignancy
25%	≤1.26	3	0.266	7	0.219	15	0.618
50%	>1.26 – 1.85	7	0.121	19	0.097	24	0.381
75%	>1.85 – 3.0	8	0.038	5	0.029	12	0.149

Abbreviations: ADC=apparent diffusion coefficient, n=number of lesions